[redacted]

CLASSIFICATION CHANGE

TO - UNCLASSIFIED [redacted]

By authority of [redacted]

Changed by [redacted] Date 6/11/74

Technical Memorandum No. 33-143

(Revision 1)

The Syncom I JPL Apogee Rocket Motor

(Title Unclassified)

R. G. Anderson

W. Gin

D. P. Kohorst

jpl

JET PROPULSION LABORATORY

CALIFORNIA INSTITUTE OF TECHNOLOGY

PASADENA, CALIFORNIA

September 16, 1963

[redacted]

[redacted]

[redacted]

CM-4279

Technical Memorandum No. 33-143
(Revision 1)

The Syncom I JPL Apogee Rocket Motor
(Title Unclassified)

R. G. Anderson
W. Gin
D. P. Kohorst

L. R. Piasecki

L. R. Piasecki, *Chief*
Solid Propellant Engineering Section

Copy No. 21

JET PROPULSION LABORATORY
CALIFORNIA INSTITUTE OF TECHNOLOGY
PASADENA, CALIFORNIA

September 16, 1963

[redacted]

[redacted]

[redacted]

Prepared Under Contract No. NAS 7-100
National Aeronautics and Space Administration

CONTENTS

TABLES

TABLES (Cont'd)

FIGURES

PREFACE

On July 26, 1963, the first successful SYNCOM I satellite was injected into a nearly circular, synchronous orbit by the firing of the first flight motor (P-46) of the design described in this Report. The altitude of firing was approximately 22,500 mi. The motor burned 19.7 sec and imparted a velocity increment of 4712 ft/sec to the spacecraft. The mission was completely successful.

ABSTRACT

The Jet Propulsion Laboratory has completed the development and qualification of a small, spacecraft-stage solid-propellant rocket motor. The motor contains 60 lb of propellant, and its mission is to lift the NASA SYNCOM I spacecraft from its elliptical transfer trajectory to a near-synchronous altitude. The motor fires at the apogee position and places the spacecraft into an inclined orbit over the Earth's equator between South America and Africa. The spacecraft is an active repeater, narrow-band, experimental communications satellite. Launch operations for the spacecraft fitted with this motor are scheduled for mid-1963.

The spacecraft is spin-stabilized to maintain attitude control and to achieve antenna directionality. Therefore, the requirements for precision of thrust vector alignment for the motor during firing and dynamic balance after firing are unique and stringent. The motor development program has accordingly focused on these special problems in the areas of case and nozzle fabrication and insulation development.

The motor case is fabricated from AISI 410 stainless steel, 0.013 in. thick in the cylindrical section. A 6A14Va titanium case weighing 36% less was developed as a high-performance backup. The propellant is a polyurethane–ammonium perchlorate–aluminum system. The

ABSTRACT (Cont'd)

grain configuration is a combination internal-burning star in the head end and tubular. The partly submerged conical nozzle is a three-piece construction, consisting of a steel ring adapter, a one-piece compression-molded macerated-carbon cloth body and exit cone, and a high-density graphite throat insert. Case and nozzle insulation is provided by an asbestos-filled nitrile rubber. Ignition is accomplished by a basket of aluminum–potassium perchlorate pellets situated at the head end using an AMR-safe pyrotechnic squib developed in this program. The motor is attached and transmits thrust to the payload through a brazed-on conical skirt at the head end fitted with four mounting studs.

As of the end of March, 1963, 52 rounds have been test fired to complete the development and qualification program. Test results show good reproducibility from JPL and AEDC firings. Motors have been subjected to the qualification test environments of temperature shock cycling between 20 and 140° F, temperature gradient conditioning at these temperatures, simulated booster vibration loads, and near-vacuum exposure, and have been fired successfully under these various and combined conditions.

The motor design, development problems, and qualification program and results are described in this Report.

Author

I. INTRODUCTION

The Jet Propulsion Laboratory (JPL) has completed the design, development, and qualification of a small, spacecraft-stage, solid-propellant rocket motor. This Report describes the end application of the motor, the chronology of the development program, the design approaches, unique development problems and their solutions, and the performance results from the qualification firings. Additional detailed data and information generated during the program are presented in Ref. 1.

A. Application

The mission of this motor is to lift the National Aeronautics and Space Administration (NASA) SYNCOM I spacecraft from its elliptical transfer trajectory to a nearly synchronous altitude at 22,300 mi above the Earth. Boost and injection into the transfer ellipse are accomplished by the three-stage launch vehicle, *Thor–Delta.* Prior to third-stage ignition of the ABL-248 rocket motor, the *Delta* stage is spun up to about 160 rpm, a rate which is maintained through apogee motor firing and after burnout. The motor fires at the apogee and places the spacecraft into an inclined orbit over the Earth's equator, projecting an elongated figure 8 between South America and Africa. The spacecraft (Fig. 1) weighs about 85 lb after apogee stage burnout. It is an active repeater, narrow-band, experimental communications satellite capable of transmitting a two-way telephone or several teletype messages (Ref. 2).

B. Chronology of Program

The spacecraft and ground synchronous control equipment were designed, developed, and fabricated by Hughes Aircraft Company under the program and technical management of the Communications Branch of the NASA Goddard Space Flight Center. Extensive prototype work had been accomplished by the spacecraft contractor, which permitted a relatively short system development program before launch. This also implied the use of, or a modification of, an existing apogee motor.

The most nearly adaptable motor for the apogee stage was the Thiokol-Elkton Division Titan vernier motor, the TE-345, a spherical 13.5-in.-diameter motor with 67 lb of propellant. Program schedule dictated the choice of this motor for early system tests and for the first flight. Design modifications were made in the case attachment, grain configuration, and nozzle, and a minimum number of motors were fabricated to qualify the modified configuration. The uncertainty in booster capability and trajectory requirements necessitated that the apogee motor be capable of off-loading from the maximum propellant load at some time during the program. Thiokol developed a novel technique for accomplishing this.

Simultaneously, the SYNCOM Program Office requested JPL to design and develop a motor specifically for this application. It was to be optimized so that a significant payload weight margin could be realized and have the capability to off-load within reasonable limits. Under sponsorship of the Office of Advanced Research and Technology of the NASA, the Laboratory conducts a continuing motor technology improvement program. Experimental and design information (such as that needed for nozzle material selection) obtained from this program was applied to the SYNCOM motor design. Work was initiated in November 1961. The motor was qualified by the end of February 1963. On the February 14, 1963 launching of the first spacecraft using the Thiokol motor, the telemetry was lost 20 sec after the apogee fire command. Because the possibility exists that the apogee stage firing produced excessive acceleration and vibrational loads on the communications electronics and wiring, additional and more extensive systems tests will be conducted with the apogee motor. Launching with the JPL motor is scheduled for the middle of calendar 1963.

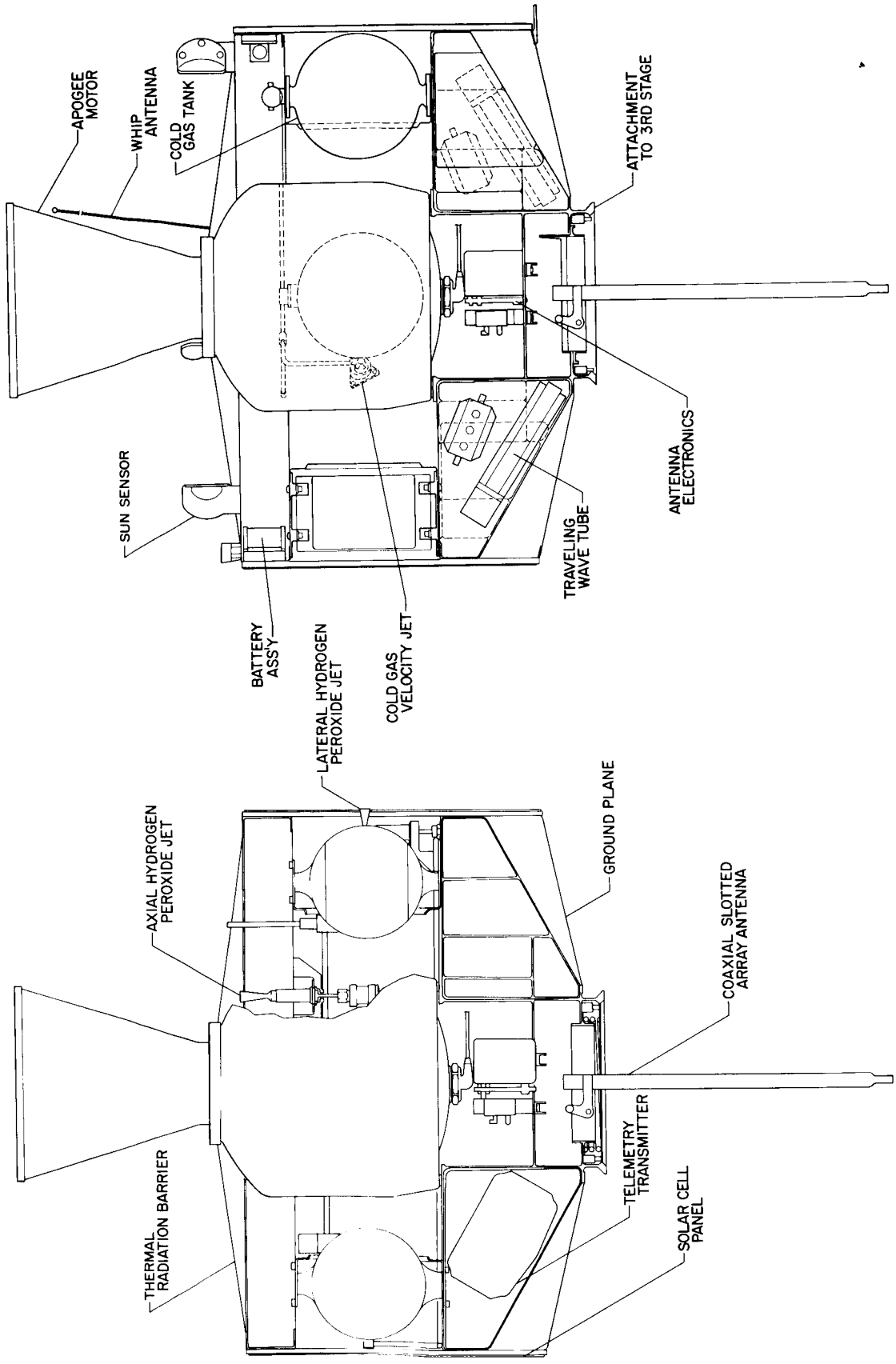

Fig. 1 Layout of SYNCOM I spacecraft with JPL motor

II. DESIGN FEATURES

A. System Requirements

The apogee motor design had the following system requirements:

1. The nominal incremental velocity required is 4841 ft/sec for a spacecraft weight (with apogee motor before ignition) up to 145 lb.
2. The motor must withstand the environmental output from the *Thor–Delta* vehicle and be spin-fired at 160 rpm.
3. The motor must be capable of off-loading to accommodate a total spacecraft weight of 125 lb.
4. The best possible reproducibility in total impulse and the minimum thrust vector misalignment should be the design and development goals.
5. The dynamic imbalance of the inert parts about the axis of spin prior to propellant loading must be within 5 oz-in.^{2}, and must not exceed this value after burnout.
6. The motor must operate reliably in a space environment of hard vacuum up to 50 hr and at motor temperatures between 20 and 130°F.
7. The motor should have a low ratio of length to diameter to minimize the spacecraft ratio of roll to pitch inertia.

The motor designed to meet these requirements is shown in Fig. 2.

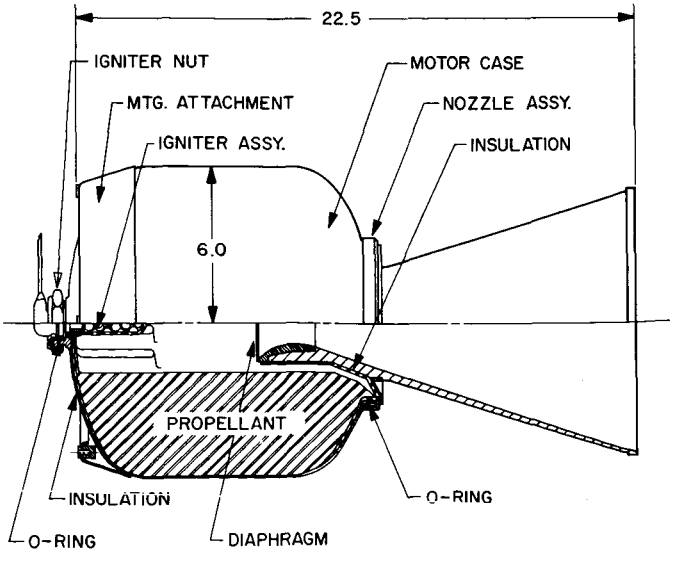

Fig. 2. Assembly drawing of motor

B. Motor Case

The motor case was designed as a short cylinder with ellipsoidal heads of 2:1 ratio. This shape was required to fit the grain configuration and to meet the inertia ratio requirements of the spacecraft. The design philosophy was to produce a motor case based on a predictable material, fabricated by well established techniques. Weight was minimized by using a small design factor on material strength and by holding very close tolerances on the shell thickness. This resulted in a case having a wall thickness of 0.013 in. and weighing 3.9 lb. The design parameters used are given in Table 1. This philosophy, coupled with a strict quality control program, has resulted in a highly reliable motor case. Of the 50 cases built, not one has failed as a pressure vessel, either in proof testing or firing, even though some have been fired and proofed as many as three times.

Table 1. Case design parameters

Parameters	
Operating pressure	280 psi
Proof pressure	290 psi
Yield pressure[a]	300 psi
Minimum material properties	
Tensile strength	180,000 psi
Yield strength	140,000 psi
Weld joint efficiency	95%

[a]Pressure at which the case reaches the proportional limit of the material under biaxial stress conditions.

Type 410 chromium steel was selected for these motors on the basis that it is reliable, readily available, easily processed, and develops a reasonably high strength. Although other materials were considered more attractive for various reasons (especially titanium), they were all discarded in favor of 410 because of high cost, poor delivery, or low reliability. The titanium approach was relegated to a backup status because the higher cost was not justifiable under the program fiscal or performance requirements.

To produce the motor case in the short time dictated by the schedule, an all-sheet-metal type of construction was chosen with welded and brazed joints. The closure domes were hydroformed, while the cylindrical section was rolled and welded. All were formed from sheet ground to thickness. The joints forming the vessel shells

were TIG-welded (Tungsten arc, Inert Gas-shielded) using specially designed tooling to maintain the close dimensional control required. The conical attachment bracket was brazed into place with a 35% gold–65% copper alloy. Final machining of the surfaces critical to thrust alignment was performed last.

Some of the unusual aspects of the case are as follows:

1. The volume of all cases was held to within 1% of one another so that each could contain exactly the same amount of propellant.
2. Because the motor was to be dynamically balanced about the spin axis, the bow and ovality of each motor were held to within 0.030 in.
3. As the thrust of the motor had to be accurately aligned with the spacecraft, the plane of the mounting bracket had to be held perpendicular to the axis of the nozzle within 0.002 in. This required extremely close tolerances between the mounting bracket and the nozzle boss.

C. *Propellant and Grain Configuration*

The propellant for the SYNCOM I motor is a composite polyurethane fuel binder, ammonium perchlorate oxidizer, and aluminum fuel additive system, carrying the designation JPL 540. The formulation is shown in Table 2. The detailed description and characterization of this propellant are found in Ref. 3. All of the fuel ingredients except the toluene 2,4-diisocynate are premixed at an elevated temperature in a 25-gal Bramley mixer. The ammonium perchlorate is then added and mixing continued at an elevated temperature. The mix is cooled to about 85°F, the TDI added, and final mixing is accomplished. All mixing and casting are carried out under a pressure of 5 mm Hg or less. The propellant is cured at 140°F for 72 hr.

Table 2. JPL 540 propellant properties

Propellant formulation	
Ingredient	**Weight percentage**
Ammonium perchlorate	64.00
Aluminum powder	16.00
Polyurethane binder	19.71
Neozone-D	0.25
FeAA catalyst	0.04
Selected physical and mechanical properties	
Density, lb/in.^{3}	0.0624
Heat capacity Cp, Btu/lbm-°F	0.296
Thermal conductivity, Btu/hr-ft-°F	0.350
Elongation at maximum stress, %	64.00
Maximum tensile strength[a], psi	142.00

[a]Measured at a strain rate of 0.74 in./in./min based on effective gage length.

Propellant batches of 275 lb are usually made to load at least three full-scale motors and several smaller quality-control motors. Flight motors are cast in triplets, so that one flight and one flight spare, plus one batch check, are available from the same batch.

Selected physical, ballistic, and mechanical properties of JPL 540 are shown in Tables 2 and 3. The propellant performance has been estimated by the performance calculation program originally developed by Aeronutronic Division of Ford using the IBM 704 computer. The theoretical specific impulse is computed for a 0-deg expansion angle and averaged between frozen and equilibrium flows. The average is based on an empirical formula which takes the difference between equilibrium and frozen specific impulse at the throat condition plus 1 sec and adds it to the frozen specific impulse at any station of interest downstream. On this basis, the vacuum theoretical specific impulse for the reference chamber pressure of 1000 psia and expansion to 14.7 psia is 256 sec. For a chamber pressure of 200 psia and expansion to 35 in vacuum, representative of motor performance conditions, it is 299 sec. The specific impulse efficiency depends on degradation due to losses from heat transfer, divergent flow, reverse flow, and particle lag.

The grain design of the motor is a combination straight cylinder and eight starpoints at the head end. The geometry is such that propellant burnout occurs in the two ellipsoidal ends prior to taking place in the cylindrical section. A sliverless condition is attained theoretically; however, unevenness of insulation and distortion of the grain and initial burning surface resulting from propellant cooldown after cure contribute to occasional chuffing.

Table 3. JPL 540 ballistic parameters

Burning rate relation	$r = aP^n$
For $P < 150$ psia	$a = 0.0112$
	$n = 0.549$
For $P > 150$ psia	$a = 0.0423$
	$n = 0.285$
K_N relation	$P = bK_N^{1/1-n}$
For $P > 150$ psia	$b = 0.295$
Temperature sensitivity	$\pi_K = (1/P)\, dP/dT = 0.00086/°F$

Close quality control of the insulation dimensions and post-cure machining of the propellant surface can eliminate the possibility of chuffing. The starpoints in the head ellipsoidal end increase the available initial propellant surface. They also present propellant surface in close proximity to the igniter as well as increasing the volumetric loading of this design.

D. Nozzle and Insulation

To minimize the pitch moment of inertia of the motor, the nozzle was submerged deeply into the chamber. This design also requires less insulation at the aft end of the case than a convergent–divergent external nozzle because of the stagnation of flow in that end. However, a disadvantage arises from the fact that, in the burned-out condition, the hot throat is located so that a large portion of the heat is retained inside the motor and thus within the spacecraft.

The nozzle is an 18-deg cone, expanded to an area ratio of 35:1. It is a three-piece construction, consisting of a steel ring adapter, a one-piece compression-molded macerated-carbon cloth body and exit cone, and a high-density graphite throat insert. The ring adapter is threaded and screwed to the case and locked with three set screws. The carbon cloth body is, in turn, threaded and bonded to the nozzle ring. The macerated carbon cloth is manufactured by National Carbon Company and is coated with a phenolic resin by Thermal Materials, Inc. The body is molded at approximately 18,000 psia and 315°F.

The leading edge of the submerged nozzle and the sonic throat region are provided by a one-piece, high-density graphite, designated ZTA, from the National Carbon Company. The material is compression-molded and heat-treated, resulting in a specific gravity of 1.92. A gradual entrance design was used in an attempt to minimize two-phase losses in that critical region. The insert is bonded to the body and is additionally threaded to provide mechanical interlocking after firing. Precision final machining is done on the nozzle attachment ring and the inside contour of the insert and exit cone to ensure geometric thrust alignment and to provide a run-out surface on the ring for motor-to-payload installation.

The nozzle ring, the joint between the body and the ring, and the nozzle body immediately aft of the throat are insulated against the combustion gases by a molded, bonded collar using a General Tire and Rubber Company material designated V-52, an asbestos-filled, acrylonitrile butadiene compound. The same material is used to insulate the case in the form of two molded boots for the ellipsoidal ends and sheet stock for the cylindrical portion. At the head end, the thickness starts at the igniter boss at about 0.19 in., tapering to 0 where the cylindrical case is met. At the nozzle end, the thickness starts at 0.16 in. and likewise gradually tapers off. The cylindrical region, needing less insulation, is covered by one layer of 0.030-in. sheet stock.

E. Igniter Subsystem

The ignition of the rocket motor is accomplished by the combustion of a basket of 60 g of aluminum–potassium perchlorate pellets (ALCLO pellets, 0.375-in. dia. × 0.195-in. thick, from Aerojet-General), in turn ignited by an electrically initiated pyrotechnic squib. The igniter assembly (see Fig. 2) is located in the head end of the chamber surrounded by the eight-pointed star of propellant. The perforated basket is a layup of eight layers of 9-mil thick 181 fiberglass in a configuration 1.40 in. in OD and 2.0 in. in cylindrical length. A hole pattern is drilled to spread the flame, and the basket survives the burning of its contents but gradually burns and erodes during motor burning. The approximate quantity of heat generated by the igniter is 140 kcal.

A moisture and pressure seal (which may improve but is shown to be unnecessary for pellet ignition) is provided by a sleeve, a few mils thick, of a molded, irradiated polyolefin called MIM-X, bonded and shrunk-fit over the perforated basket.

The dual-bridgewire igniter squib is a new development which meets the motor requirements as well as the Atlantic Missile Range safety requirements against stray current ignition of squibs by withstanding a 5-min exposure to 1 amp and 1 w without autoignition (see Sect. III E and Ref. 4). The squib body has a circular plate, which serves as the igniter and case head-end cap as well as passing pressure lines for static test gages.

Space limitation and mounting restrictions in the payload dictated the design of the squib cable, as shown in Fig. 2. A permanent pigtail connector is potted to the squib and led out by a cable with a Cannon connector to the power supply. The squib body design required that the cylindrical portion housing the bridge wires and the pyrotechnic material be inserted into the basket to minimize the external length of the igniter. This was a late development, which led to the rather inefficient use of stuffer rings to keep the pellets well packed and forward of the squib firing end.

III. SPECIAL DEVELOPMENT PROBLEMS AND SOLUTIONS

A. Motor and Thrust Alignment

To minimize undesirable precession of the spinning spacecraft and corrective controls requirements after apogee boost, the motor thrust misalignment is kept at a minimum possible value. Tolerances are also very tight to permit good balance and alignment when the apogee motor is mated to the payload. The approach taken on this development was to design and fabricate with as much precision as feasible all parts of the motor and then to determine from static tests to the degree possible what thrust misalignment may exist and is measurable during firing.

Precision machining and inspection procedures are adopted on those case and nozzle parts that affect alignment (including casting mandrel alignment) and balance. Both the nozzle and the case are inspected at the respective manufacturers and are critically examined separately and together as an assembly at the Laboratory. The Cleveland Instrument Company "INDI-RON," a precision roundness, concentricity, and squareness electronic gage, is used for final inspection. The parts are rotated on a precision spindle while the gage remains stationary.

Case self-alignment is determined by placing the *B* surface of the chamber (Fig. 3) on the rotating surface of the gage and bringing the *A* surface to alignment with the spinning axis. The head-end inside diameters *C* and *D* are read for roundness and concentricity. Then, the parallelism of the surfaces of the four mounting studs is checked with reference to the surface *B*.

The selected nozzle is next mated securely to the case, and the assembly is inspected (Fig. 4). Precision flat blocks mount the assembly to the rotating table. The concentricity of the *H* surface (a runout surface also used for mating the loaded motor to the payload) is optimized with respect to the rotating axis. The concentricity and roundness of surfaces *G*, *F*, and 7 are then read to yield the value for nozzle geometric alignment.

The insulated case and nozzle assemblies of two flight-type motors (serial numbers P-46 and P-55) produced at the end of the development program had the following inspection records:

1. Nozzle misalignment (defined as the nonconcentricity of throat plane *G* and exit plane *F* divided by

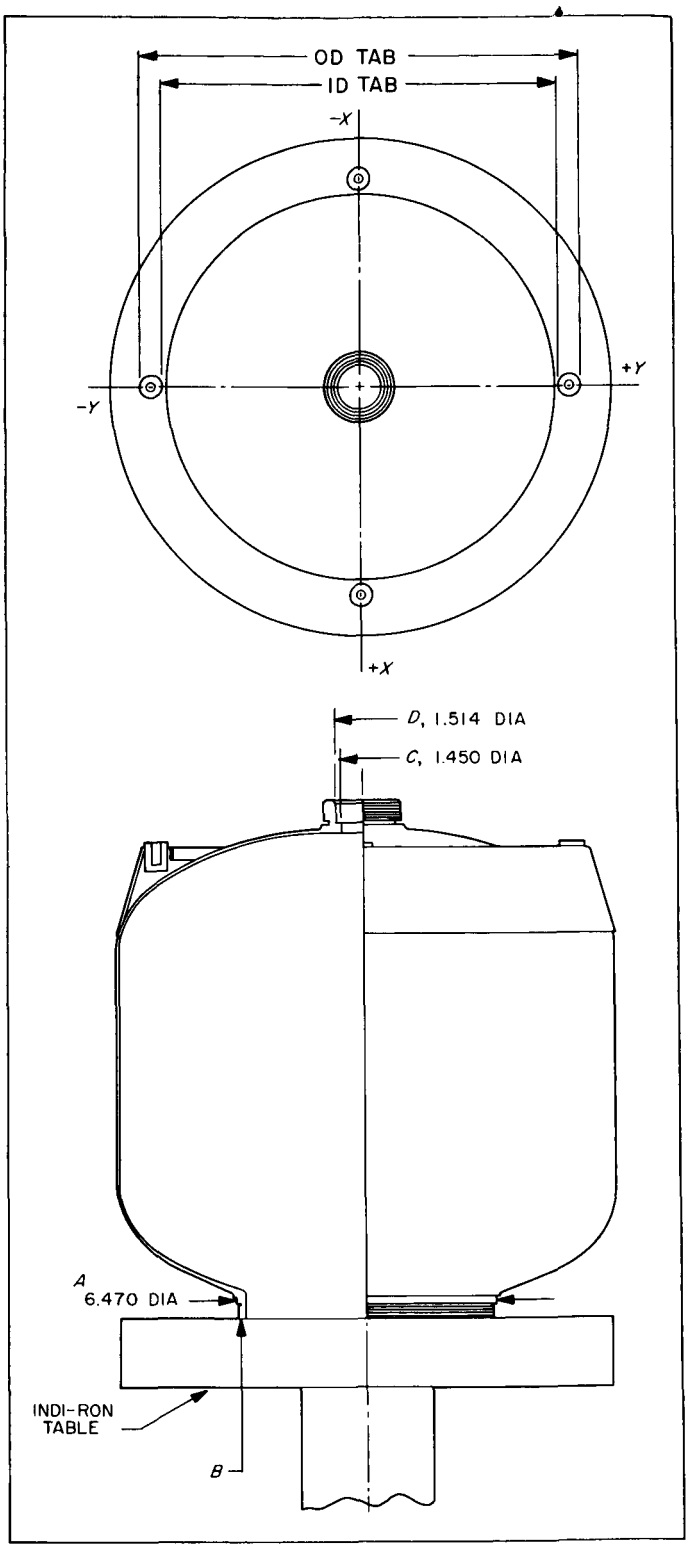

Fig. 3. Chamber inspection procedure

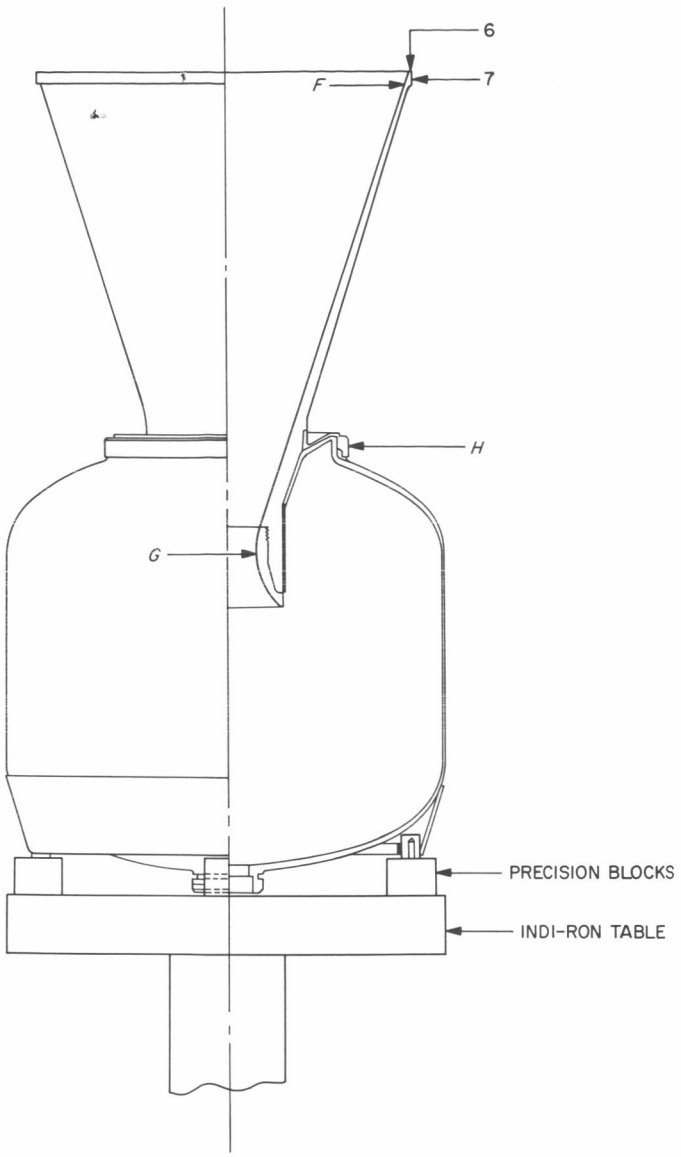

Fig. 4. Chamber-nozzle inspection procedure

the distance between the two planes) was 0.0001 in./in. for both assemblies.

2. Thrust offset (defined as the distance between the center of the attachment plane and the point of interception of that plane and the nozzle centerline which connects the centers of throat plane *G* and exit plane *F*) was 0.0012 in. for P-46 and 0.0006 in. for P-55.

3. The out-of-roundness of the runout surface *H* was 0.0005 in. for P-46 and 0.0011 in. for P-55.

4. The maximum out-of-flatness of the attachment pads was 0.00035 in. for P-46 and 0.00034 in. for P-55.

To determine the possible effects on the alignment after propellant loading, the following procedures were followed: The motor assembly (comprised of case number P-41 and nozzle number F-54) was critically inspected for alignment. Next, the insulated case and nozzle assembly was dynamically balanced by the proper addition of balance weight (see Sect. D), and then the case was loaded with propellant using inert oxidizer. A check of the reassembled unit showed that the processing of the propellant grain caused only minor changes in the alignment (and dynamic balance), and both dynamic imbalance and misalignment were still within the maximum allowable.

With such precision alignment fabricated into the motor, the motor can be installed into the payload very exactly. In fact, the individual cases and nozzles are so precise that units can be assembled at random, and extremely close nozzle centerline to attachment plane can still be achieved. During operation, there would be minimal or zero net side forces. Partial experimental confirmation was obtained from static tests of motors with shortened nozzles on a six-component stand enclosed in a zero-flow ejector assembly (Figs. 5 and 6). Since the chamber-pressure–time curve is progressive, the critical operation of a zero-flow ejector occurs during the early portion of the run at the lowest chamber pressure. The average chamber pressure of the motor is also relatively low, being about 200 psia. It was necessary to obtain full-

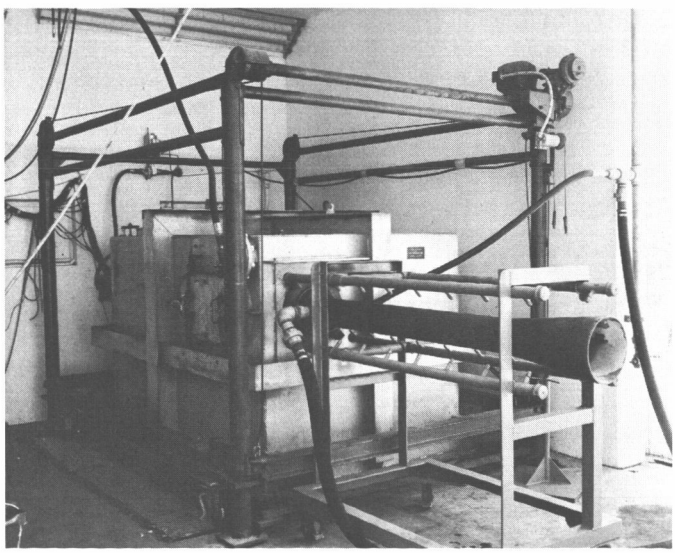

Fig. 5. Zero-flow ejector enclosure over six-component stand

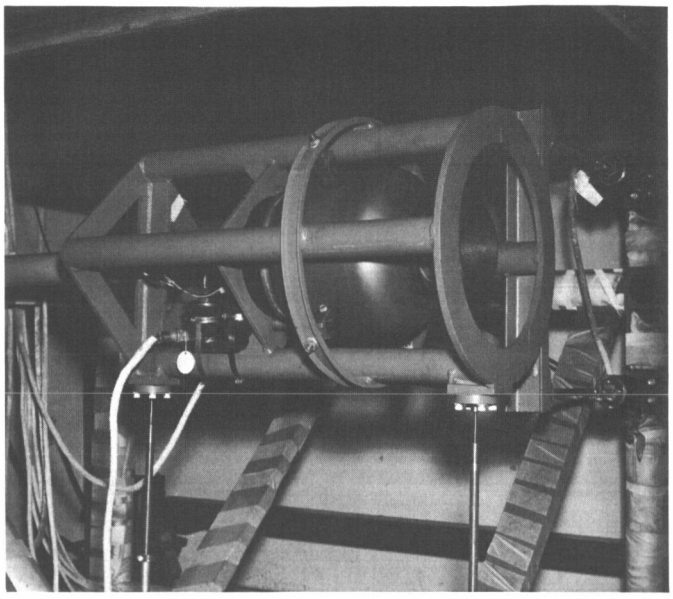

Fig. 6. Cradle with motor on six-component stand

flowing nozzles for the entire firing duration (excluding motor tailoff) to record side forces reliably. A straight tube ejector was designed with a diameter of 5.75 in. which accommodated a nozzle expansion ratio of 7.8 (compared to 35 for flight). At ambient conditions, the nozzle flows full from motor ignition. Ignition transients caused by the dynamic response of the thrust stand are dissipated after approximately 0.35 sec of motor operation.

The thrust stand is calibrated by applying static loads in various directions and determining the interaction of the thrust measuring legs. As a result of these calibrations and past experience with this stand (Ref. 5), the side force measuring capability is accurate to ± 1 lb of force. The results from the six tests showed that there were no detectable side forces outside of the resolution limits of the stand.

Nozzle throat area increase due to erosion measured after static tests has been recorded in the range from 0.5 to 1.5%. The pattern is very symmetrical and should not cause measurable unbalanced side forces. (The apparent irreproducibility of total erosion is believed to be the result of the variation in erosion resistance of the graphite billets. Since the material is compression-molded, there is probably a batch-to-batch variation in mechanical properties.)

B. Motor Case Testing

The qualification vibration test levels required for the motor are shown in Table 4. Motors loaded with physically and mechanically similar but inert propellant were supplied to the satellite contractor, Hughes Aircraft Company, for dynamic model testing. The motor was mounted to the satellite, and accelerometers were mounted in appropriate stations to record gains and resonant frequencies.

Table 4. Qualification vibration test levels

Frequency cps	Acceleration level g rms	Time duration min
Axial direction—sinusoidal sweep		
5–50	1.5	1.74
50–150	7.5	0.81
150–230	87.0	0.33
230–500	7.5	0.58
500–2,000	15.0	1.04
Lateral direction—sinusoidal sweep		
5–50	0.6	1.74
50–160	3.0	0.86
160–300	5.3	0.50
300–500	1.5	0.36
500–2,000	3.0	1.04

During the first vibration test performed at these levels, several fatigue cracks were discovered in the motor attachment bracket of the initial case design. Examination of the data disclosed that the gains at the motor–spacecraft interface were higher than predicted. There also appeared to be some resonant coupling. Steps were taken immediately to redesign the bracket, increasing its strength and stiffness. The conical skirt mount resulted (Fig. 7). Subsequent tests showed that the design objectives had been met. The natural frequency of the motor was raised from 255 to 325 cps. This was sufficient to decouple it from the spacecraft structure. No other vibration problems have been encountered.

Three motor cases were subjected to a hydrostatic burst test to determine whether design objectives had been fulfilled. Two units selected had been fired previously, and one was as manufactured. The data given in Table 5 show results which are unusually close to the design values. It is normally difficult to come this close, as the strengthening effect of a biaxial stress condition is hard to predict accurately.

C. Titanium Motor Case Development

A titanium version of the SYNCOM I motor case was developed as a possible high-performance backup for the

Table 5. Hydrostatic burst test data

Serial No.	Yield pressure, psi	Burst pressure, psi
B1X	300	456
P68	339	483
P69	328	422

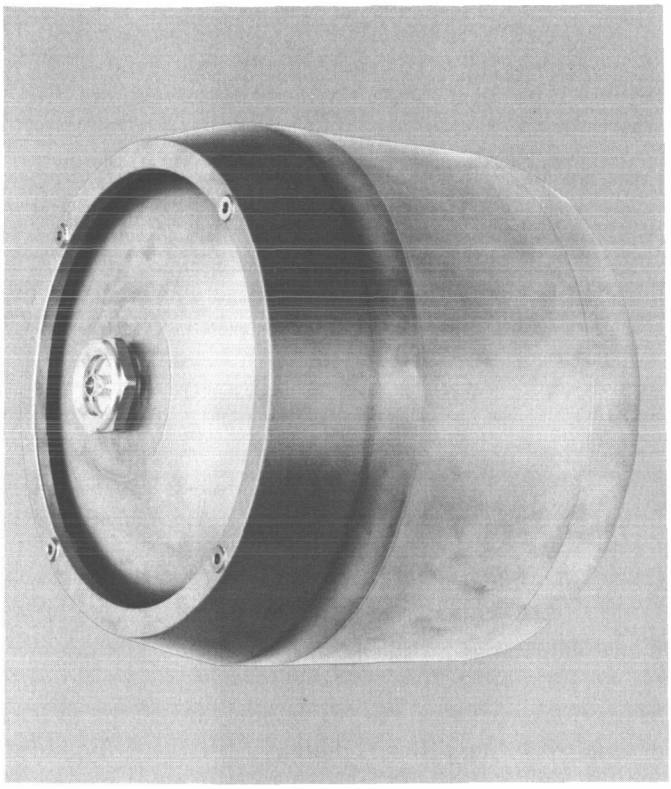

Fig. 7. Flight case with redesigned mounting bracket

type 410 steel case. By fabricating from the titanium 6% aluminum–4% vanadium alloy heat-treated to a minimum yield strength of 150,000 psi, it was possible to reduce the case weight by 36%. The total weight of the titanium case is 2.5 lb.

This case was designed to be manufactured by a considerably different method from that used on the type 410 units. Basically, it consisted of welding together three machined forgings. Two of the forgings, bell-shaped and nearly identical, make up the shell of the vessel; the third is for the mounting ring. The shell forgings, originally 0.5 in. thick, are carefully contour-machined inside and out to the required 0.013-in. wall thickness. The ring is machined from a conical forging, slightly thicker than the shell forging. The three pieces are then welded together by the electron beam process. Final machining of the mounting surfaces finishes the case.

This type of fabrication is desirable for very high-strength materials, as it minimizes the amount of welding required and eliminates the highly stressed longitudinal joint as on the roll-formed 410 case.

The major disadvantage of this motor case is that its cost was about twice that of the type 410 unit.

Burst test results show that this design also has good reliability. The test indicated a yield point (pressure at which the case reaches the proportional limit of the material under biaxial stress conditions) of 365 psi and a burst pressure of 535 psi.

Three cases were loaded as qualification motors and subjected to temperature cycling between 20 and 140°F. One each was then fired at 20, 80, and 140°F, with internal vacuum applied before ignition. All motors performed successfully, and post-fire visual inspection revealed no abnormal hot spots or other deformities.

D. Dynamic Balance

To maintain spin stability throughout the mission, stringent balance requirements are placed on the motor before and after burnout. The allowable dynamic imbalance about the axis of rotation of the motor in the spacecraft assembly is 50 oz-in.^{2} After burnout, the allowable dynamic imbalance about the same axis is 5 oz-in.^{2} Whereas static imbalance alone shifts the axis of rotation, dynamic imbalance causes a wobbling detrimental to the spinning mode of operation of the antenna.

It is generally not possible to have the motor in dynamic balance both before and after propellant expulsion. The more critical condition regarding balance is after motor burnout. Therefore, the procedure is to bring the motor hardware to dynamic balance before the loading of propellant. For this purpose, a standard Gisholt 3S Dynetric balancing machine was used (Fig. 8). The motor assembly, less the ignition system, which is located on the centerline, is supported horizontally by a shaft with a tapered plug at the nozzle throat and a head-end plate to which the assembly is bolted at the attachment pads. Static and dynamic balance are achieved in one operation.

Slugs (1/16 or 1/8 in. thick) of a lead–zinc alloy are used as balance weights adhered permanently to the motor

surface with an epoxy resin (Eccobond 45). The minimum balance weight requirement would result if the largest radius of the case were the location for the weights. The maximum radius is the cylindrical portion, which, however, may become so excessively heated in spots after motor burnout as to soften an epoxy bond. Cooler areas were selected instead. In the meantime, the lead–epoxy-case bond was subjected to thermal shock tests (ambient temperatures of 20 to 140°F) in simulated vacuum with applied loads, without any indications of weakening.

The two balance planes selected are located on the conical attachment skirt, 0.8 in. aft of the attachment pad surface and on the exterior inner surface of the nozzle ring, 12.1 in. from the attachment pad surface. The lead balance weights, their location in azimuth as well as distance from the assembly center of gravity, and their distance from the assembly centerline are recorded. Since the balancing weights are much smaller than the weight of the balanced assembly, their effect on moving the assembly center of gravity is neglected. It is then possible to calculate separately, by algebraic analysis or graphical vector analysis, the amount of static and dynamic imbalance removed by the addition of the balance weights.

Two initial tests were made of motors for which the hardware had been balanced prior to propellant loading and firing at the simulated altitude facility at the Arnold Engineering Development Center. After firing, over 200 g of charred and detached insulation were removed from each motor. The remaining insulation, a silica-filled butyl rubber (Stoner Company), although serving as case insulation very effectively, was unevenly distributed and had very little structural integrity. The post-fire check of balance without the 200 g of residue showed one motor (Test AEDC-07) to have a dynamic imbalance of 12 oz-in.^{2} and the other (Test AEDC-08) to have an imbalance of 3 oz-in.^{2}

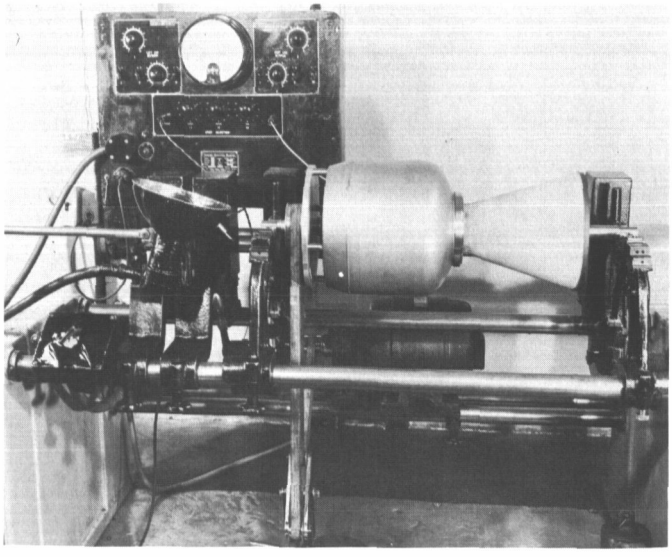

Fig. 8. Empty motor case and nozzle on Gisholt balance machine

The above numbers indicate that the 5 oz-in.^{2} post-fire requirement may not be consistently met, if at all. The primary cause of insulation deterioration is the hot throat insert, which, having passed about 60 lb of 5700°R combustion products, now transfers radiant heat to the surrounding insulation and cooks it. One approach used to minimize loose insulation material was to increase the thickness of butyl in an attempt to preserve a better bond and maintain some virgin material between the charred insulation and metal. The balance results from this test were inconclusive, indicating no measurable improvement. Simultaneously, a screening test using an acetylene torch on sample materials demonstrated that the butyl rubber does not have nearly the char strength to withstand post-fire heat and agitation shown by an asbestos-filled nitrile rubber (GT and R Company). This material had been tested and used in another JPL advanced technology program. The heat conductance of the two materials is essentially identical. The decision was then made to switch materials. A thicker insulation was also adopted for several reasons. Two tests made to compare the thin versus thick nitrile rubber insulation showed the thicker material to be in better condition after the firing. Also, since the spacecraft did not have overweight problems, it was convenient to off-load to the correct amount of propellant by using the heavier case insulation. Finally, spacecraft thermal control after apogee motor burn turned out to be a more serious problem than originally anticipated, and the heavier insulation served to keep the case temperature lower.

Three subsequent tests showed the improvement in dynamic imbalance. Test E-42 was conducted on the spin-fire test stand at the Laboratory's test station at Edwards Air Force Base. The post-fire motor (less 180 g of charred loose insulation) was checked on the balance machine and showed a static imbalance of 2 oz-in. and a dynamic imbalance of 6 oz-in.^{2} Two tests at the AEDC showed 1 and 3 oz-in. static imbalance and 2 and 1 oz-in.^{2} dynamic imbalance, with 160 and 150 g of loose material, respectively, removed prior to the balance checks.

It is impossible in a static or spin-fire test to determine accurately the amount of post-fire imbalance with avail-

able test equipment. The presence of Earth gravity and the handling of burned hardware (removal from test location, transportation, setting up in balance machine) cause the loosening and nonsymmetric redistribution of much of the charred insulation. Static horizontal tests at the AEDC result in more charring on the top side case insulation, while spin-fire tests at the Edwards Test Station in the vertical position result in the dropping of aft-end insulation onto the head of the end case.

It is believed, however, that in application in free space what loose material there may be will be evenly distributed by centrifugal force, and there should be no bias in the quality and physical condition of the post-fire insulation. Available test results show that the dynamic balance requirement has been substantially met after this development program.

An additional problem briefly investigated was that of the evaporation of insulation over a period of time in the space environment, which may lead to imbalance of the spinning payload. Samples of slightly charred and heavily charred insulation were placed in a 9×10^{-6} torr vacuum system at room temperature. The samples were removed and transported in a desiccator to be weighed from time to time for periods of up to about three days. Charred material showed no measurable weight loss; presumably, most of the vaporizable material had been cooked off during the firing or immediately thereafter. Using the conventional equation for evaporation of materials in space,

$$W \sim ap\left(\frac{M}{T}\right)^{1/2}$$

where

W = the weight loss rate

a = the material surface area

p = the vapor pressure of the material at temperature T

M = the molecular weight of the material

the weight loss rate for the slightly charred nitrile rubber was 6.3×10^{-6} g/cm^2-hr.

For evaporation of materials from within the fired rocket motor, the controlling area factor is the throat rather than the surface area of the charred insulation, which is large compared to the former. The Clausing factor to account for molecular reflections inside the chamber is estimated to be 0.55. Using values for $p(M)^{1/2}$ derived from the above experiments, and assuming a spacecraft equilibrium temperature of 275°K, it is estimated that the in-space loss of charred insulation will be negligible: no greater than 0.5 g a year.

E. Squib Development

A new squib was developed in order to conform to the integral igniter design as well as to comply with the 1-amp, 1-w for 5 min no-fire requirement of the AMR. The squib is manufactured by Special Devices, Inc., who originally conceived the method to dissipate stray currents. Development testing was done both at the Laboratory and at SDI. Details of the design, development, and qualification programs on the Squib are presented in Ref. 5; only pertinent highlights are given here.

To obtain reliability in redundancy, two ignition bridgewires were designed into the squib (Fig. 9). Each bridge wire or circuit must pass the no-fire requirement separately. The dissipation of 1 w in each circuit for 5 min is made possible by placing a pin bridge wire across an insulator on each pin. The pin bridge wire is surrounded by a potting compound which acts as a heat sink. Beaded ignition bridge wires are then placed across the ends of pins A-D and B-C to form two parallel circuits of three resistors each. The resistances are controlled such that, if a circuit dissipates 1 w, no more than 0.4 w is dissipated across the beaded bridge wire imbedded in the heat-sensitive pyrotechnic.

The squib qualification program involved the testing of the squib as a motor subcomponent for reliable performance after temperature shock cycling, booster vibration and acceleration loads, and simulated vacuum exposure. Of special interest is the series of all-fire and no-fire reliability tests. The squib manufacturer carried out a Bruceton analysis, using 21 squibs to evaluate the all-fire and no-fire current levels. Before the Bruceton firings, the squibs were subjected to a sequential series of tests in which the resistance was recorded, the squibs then temperature-cycled and jolted, resistance rechecked, squibs vibrated, resistance rechecked, and Bruceton-tested with a metered variable resistance circuit.

The Bruceton analysis of the squibs tested shows a 99.9% reliability at the 95% confidence level, maximum no-fire current of 1.25 amp per circuit. This corresponds to a power dissipation of 1.5 to 2 w per circuit for 5 min, which places the squib well above the AMR minimum safety requirement.

The analysis also shows, conversely, an all-fire condition at a 99.9% reliability and at the 95% confidence

level with 2.47 amp per circuit. This is well below the nominal available current from the payload power supply of 4.5 amp per circuit for apogee motor squib ignition.

At 4.5 amp per circuit, the squib delay time (time from current initiation to peak pressure measured in a closed 1.77-in.^{3} chamber) is of the order of 15 to 20 msec.

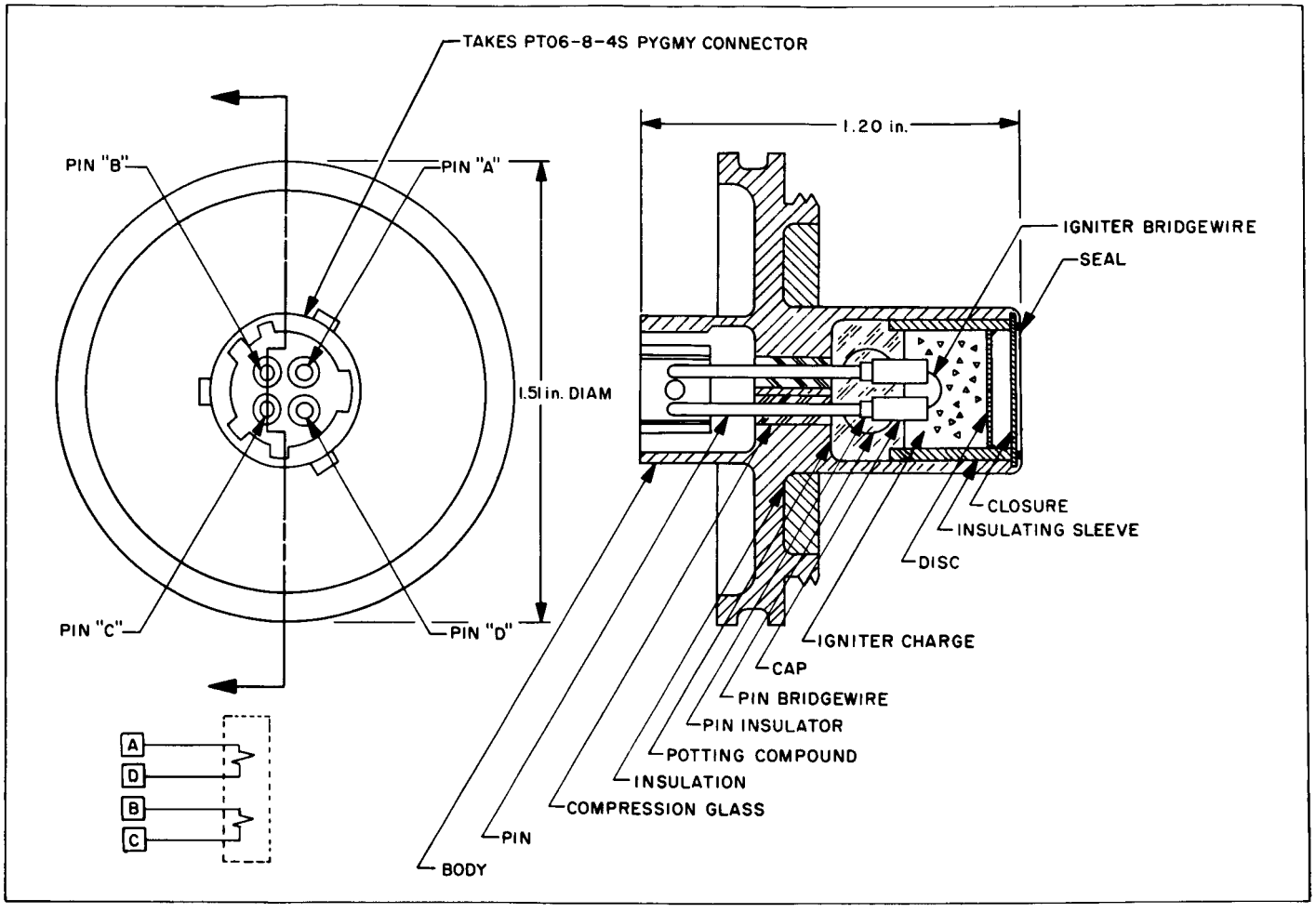

Fig. 9. Squib design

IV. MOTOR TESTING AND PERFORMANCE

A. Numerical Summary of Tests

Except for a few possible additional tests to study motor–payload interactions, the motor has been put through complete development and qualification schedules. The total number of test firings as of the end of March, 1963, is 63. Of this number, some were predevelopment tests using heavy-wall chambers, prototype igniters, and nozzles to determine general hardware and propellant performance. Of the remaining 56, three were test firings to prove the high-performance titanium backup case and one was a full-scale batch motor check from the same batch cast for the first flight motors. Two additional storage motors will be fired to make a total of 54 development and qualification rounds. The firings are generally categorized according to test objectives in Table 6. Flight-weight cases were used in all tests, and reclaimed cases were fired in some tests, although none were reused for the qualification rounds.

Table 6. Summary of development and qualification test firings

Test objectives	Number of tests
Environmental testing	
Temperature cycling, temperature gradient, simulated vacuum ignition	16
Booster vibration loads	2
Spin-fire	2
Long-term storage	6
AEDC testing	
Preliminary performance	8
Final qualification	2
Six-component testing	
Preliminary performance	4
Final qualification	4
Development of insulation to improve balance	5
Off-loaded testing	2
Contingency testing	3
TOTAL	54

B. Environmental Testing

A series of 16 motors formed a set to determine whether the motor survives and operates as planned after exposure to various temperature conditions. The motor is qualified between and including the temperature limits of 140 and 20°F. Two tests of this series were repeated because of instrumentation power failure midway through one test and because of a case burnthrough owing to an inadequate bond between case and insulation near the head end. A switch was made from 40 to 60 g of aluminum potassium perchlorate during this series to forestall low-temperature hangfires indicated in an auxiliary ignition motor test program. Subsequently, the pellet formulation was changed to yield a lower burning rate following an indication from the first diffuser test that overpressurization was occurring. Apparently a marginal design, the nozzle ring popped outward in this test but did not otherwise affect the motor performance. Accelerometer and mechanical impedance information was also obtained during the environmental tests.

Temperature cycling was done between 140 and 20°F and vice versa for 24 hr. Gradients were introduced by conditioning the motor at one extreme temperature to equilibrium and placing it at the other temperature extreme for 1½ hr. Vacuums of a few millimeters of mercury were pulled internally for 48 hr on the motor under conditioning at the high and low temperatures. Two development motors with the final attachment design were vibrated on a 5000-lb shaker to simulate axial and lateral loads anticipated from the booster acceleration. The 20 g rms at 550 to 650 cps arising from the oscillatory burning of the third stage were also simulated. Visual inspection showed no damage to the motors, which were afterwards fired successfully, one at 140 and the other at 20°F.

Spin-fire tests with the motor in the vertical position were made at the Edwards Test Station (Fig. 10). Prior to ignition, the spin motor was brought to an operating speed of 167 rpm. The spin-table drive continued to operate during the firing. The spin rpm remained constant throughout the run within the measurement accuracy of the tests. Motor chamber pressure was measured by two Taber gages mounted on the spin table. Pressure readings were taken from the spin rig through a slip-ring unit and recorded on both digital and analog systems. The effect of spinning on the accuracy of pressure-gage readings was checked in some preliminary tests and was negligible. The average characteristic velocity from pressure measurements from spin tests is identical with that from static tests within 2 ft/sec, with essentially identical dispersions of 0.4% (1 σ). Therefore, spin is believed not to affect motor ballistic performance.

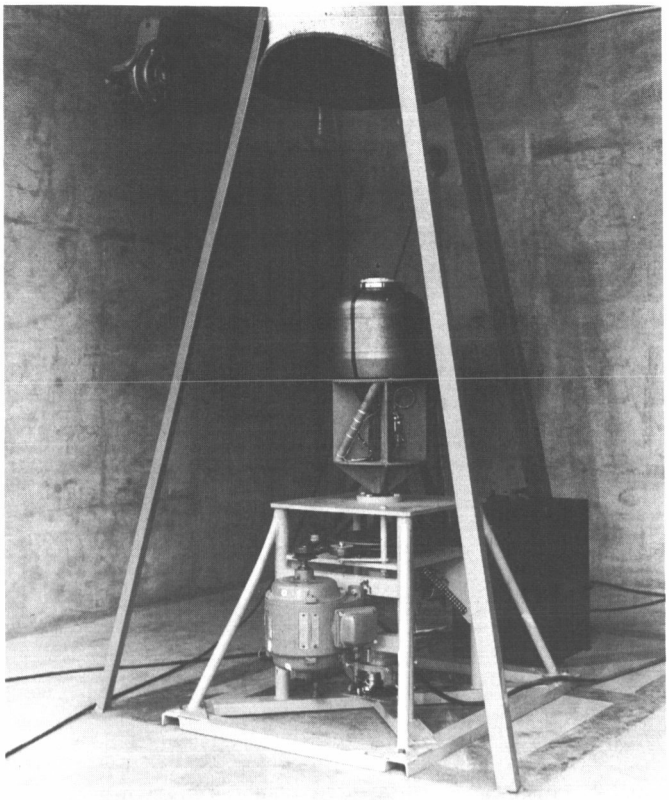

Fig. 10. Spin-fire test installation at Edwards Test Station

In order to determine whether aging upon storage affects motor performance adversely, a group of six motors was set aside under controlled conditions. Four have been fired after 6, 10, and 15 weeks, and 6 months with normal performance. All motors were conditioned to 20°F and internally evacuated to a few millimeters of mercury before ignition. The last motor will be fired 18 months from the date of manufacture.

C. Performance Testing Program

The philosophy adopted for performance testing may be summarized as follows:

1. Obtain early confirmation of vacuum total impulse from firings at the Rocket Test Facility at the AEDC, Tullahoma.
2. Conduct environmental development testing using shortened nozzles in open-air firings at JPL.
3. Obtain data on nonaxial thrust components, vibrational output during burning, and effect of spin-fire on motor performance at JPL.
4. Conduct final environmental qualification testing using zero-flow ejector and six-component stand at JPL.
5. Obtain final performance data from tests at the AEDC.

The above approach made the best use of facilities available for this program.

D. AEDC Testing

A total of ten motors were fired in the T-3 and T-4 test cells of the AEDC Rocket Test Facility. Nozzle diaphragms were ruptured for the tests to expose the grain to the low starting pressure. Average cell pressure was maintained at about 0.1 psia during the tests to allow the nozzle to flow fully to an expansion ratio of 35. Instrumentation normally included two channels of chamber pressure, four channels of thrust (two dual-load cells in series), and channels for motor case temperatures and cell pressure and temperature. Three post configurations were tested in the AEDC series. These represent the final flight configuration plus two off-loads which were considered as possible flight configurations early in the program. The flight design has the combination star and tubular perforation, while the off-loaded designs were simply two sizes of straight tubulars. An effect of load of propellant on specific impulse is apparent from these tests. It appears that the higher average L^* of the smaller propellant loads, which also means a decreased reverse velocity effect between the grain and the submerged nozzle, leads to increased performance. Table 7 shows a summary of specific impulse versus loaded weight and also indicates the degree of reproducibility of performance attained.

Late in the development program, the post-fire radiant heat transfer from the rocket motor appeared to be a more serious problem than originally anticipated. The electronics of the payload is largely situated just forward of the head end of the motor and is susceptible to overheating if the external forward end of the motor becomes too hot. The last two AEDC tests had thermocouples in various locations in the head end to check case temperatures under conditions in which the convective heating by ambient air is minimized. The data showed that case temperatures do not rise until after burnout and that a portion of the case may reach as high as 560°F about 130 sec after burnout. Details of the AEDC tests are described in official reports by the Rocket Test Facility (Ref. 6).

Table 7. Summary of test results

AEDC altityde test results, $\epsilon = 35$ (firings at 80°F)				
Configuration	No. tests	Avg. prop. wt. lb	Avg. I_{sp} [a] sec	σ %
Fully off-loaded	1	52.6	275.6	....
Medium load	4	58.2	275.6	0.21
Flight load	5	61.3	274.1	0.26

JPL diffuser test results, $\epsilon = 7.8$		
Test number	Temperature conditioning	I_{sp}, sec[a,b]
X-1365	24 hr at 80°F	251.1
X-1366	24 hr at 80°F	251.2
X-1431	Cycled between 140, 20, 140°F 24 hr each and 2 hr at 80°F	251.8
X-1432	Cycled between 20, 140, 20°F 24 hr each and 2 hr at 80°F	249.1
X-1433	Same as X-1431	251.2
X-1434	Same as X-1432	248.6

[a]Based on weight of propellant loaded.
[b]Average $I_{sp} = 250.5$ sec, $\sigma = 0.5\%$.

E. Open-Air Testing at JPL

The open-air testing at JPL, where the atmospheric pressure is about 28.9 mm Hg, required nozzles cut back to an expansion ratio of 5.1. The nozzle flow separates for the first 5.6 sec of burning if the motor is conditioned at 80°F. To correct the measured thrust during this early period as well as the tailoff to vacuum conditions, the data-reduction program which operates on digital information acquired during the firing was modified as described below.

It is assumed that the ratio of vacuum thrust to motor chamber pressure, Ku_v, is essentially a constant when the nozzle is flowing full, regardless of the degree of over- or underexpansion. The constancy is not absolute because the motor chamber pressure used for the Ku_v calculation is measured at the head end rather than at the nozzle inlet. The ratio Ku_v is very sensitive to small changes in throat area. The throat is coated with aluminum oxide during the first 12 sec or thereabouts. This is demonstrated by the low Ku_v value for various nozzle expansion ratios shown in Fig. 11, where Ku_v is plotted against $\int Pdt$. This was also confirmed by examination of a nozzle that failed early in a firing of a heavy-wall motor. Figure 11 demonstrates the essentially constant value of Ku_v, except for the coated-throat periods, for runs 1265 and AEDC-02, in which the nozzle flows full. By contrast, runs 1263 and 1317 clearly show the effect of flow separation at the beginning low-pressure portion of the tests. Run 1263 shows the separation effect at the tailoff portion of the run. When nozzle flow separation occurs, Ku_v will be greater than that for a full-flowing nozzle if the constant exit area of the nozzle is used to calculate the $PoAe$ term to obtain vacuum thrust. Therefore, to correct for the separation effects, the value of Ku_v immediately adjacent to the separated initial and tailoff portions is extended backward and forward, respectively, to calculate the vacuum thrust, now simply the product of the Ku_v and chamber pressure.

A statistical summary of the specified impulse and characteristic velocity from the open-air tests of motors with expansion ratios of approximately 5.1 is presented in Table 8. The specific impuse is the integral of total vacuum impulse calculated by the Ku_v described above, divided by loaded propellant weight. The c^* data prove to be a less reproducible indicator of ballistic performance than the specific impulse. This may be due to the complications of the two-phase flow such as the throat coating of aluminum oxide and the subsequent spalling off. The measured statistical variation of specific impulse indicated in Table 8 is representative of the state-of-the-art capability to manufacture reproducible solid rocket motors.

F. Qualification Firings with Diffuser and Six-Component Stand

A series of four motors, identical to those of the final flight configuration in all respects except for having a smaller nozzle expansion ratio of 7.8, were fired using the stand and diffuser assembly previously described. Each of the four motors was subjected to a sequence of environments, including simulated booster acceleration and vibration loads, and temperature-cycled between 20 and 140°F. Two of the motors also were subjected to

Table 8. Statistical summary of open-air tests (corrected vacuum I_{sp})

No. tests	Motor temperature °F	I_{sp} [a]		c^* [b]	
		Avg. value sec	1 σ %	Avg. value fps	1 σ %
10	20	244.5	0.35	4,936	0.38
2	80	245.0	0.13	4,959	0.49
6	140	246.3	0.35	5,004	0.39
18	20 to 140	245.2	0.47	4,961	0.74

[a]Based on weight of propellant loaded.
[b]Based on head-end pressure integral.

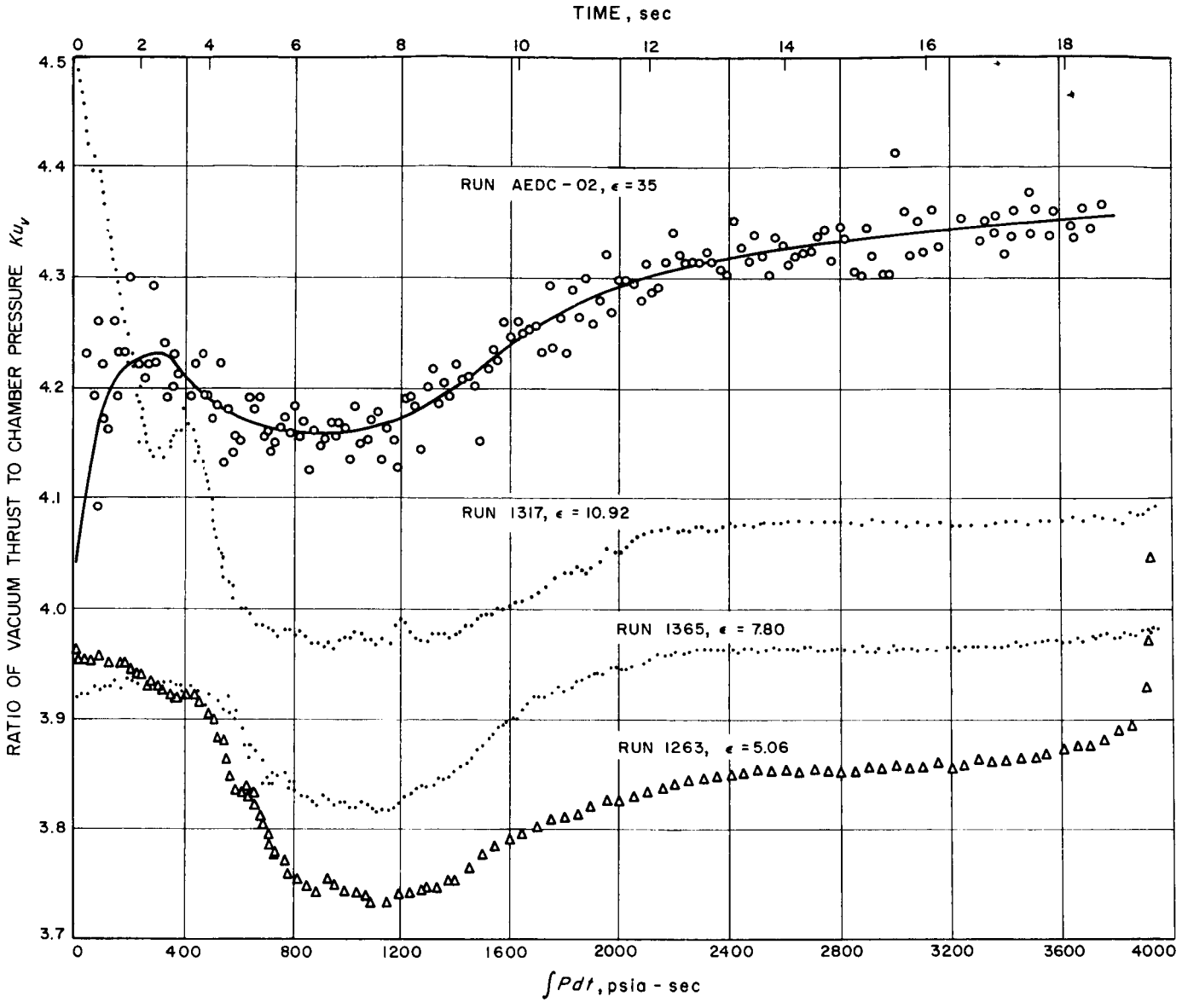

Fig. 11. Ku_v vs. burning time and pressure integral for four tests

internal vacuum during temperature cycling, which, however, is not a realistic environment. The motors were then inspected radiographically for voids, cracks, or separations. They were next conditioned to the high or low temperature and, while being installed for testing at ambient temperature, acquired a temperature gradient.

All motors fired successfully, and the measured specific impulse is compared with two earlier developmental tests of the same basic design (see Table 7). As indicated, the measured 1-σ standard deviation for all six tests over the range of temperature conditions is 0.5%. This does not account for the instrumentation error, which may contribute 0.25% on a statistical basis. In addition, the side forces measured were within the resolution of the stand and associated recording system.

G. Static Test Vibration Measurements

During the development program, the vibration output from several static firings was measured in order to

1. detect the possible presence of incipient or fully established oscillatory combustion;
2. assess the usefulness of vibration data taken during firings with the diffuser enclosure;

3. measure the vibration environment caused by motor combustion.

Data were taken from four open-air firings using a hard stand, one diffuser test using a hard stand, and one diffuser test using a soft stand. The fundamental resonant frequency of the soft thrust stand was about 15 cps at ignition and 30 cps at burnout.

Microphone data show that the intense acoustic field surrounding the motor during the four open-air firings was reduced by 36 db when the diffuser enclosing the entire thrust stand was used (from about 140 to 104 db, 0.0002 μbar). The reduction in sound pressure level was reflected by the reduction in measured vibration levels. The four open-air tests showed an average wide-band (10,000 cps) vibration level of 5.5 g rms, while the same vibration level during diffuser firings was less than 0.5 g rms. The use of a soft thrust stand also resulted in a reduction of measured vibration levels by a factor of about six in comparing the two diffuser tests.

The vibration output measured during both diffuser runs was very low both in wide-band levels and spectral peaks, thus indicating that when firing in the vacuum of space, the motor will not produce a significant vibration environment. Further, during all six firings, there were no quasi-sinusoidal vibrations to indicate oscillatory combustion. More details concerning the vibration studies accomplished during this program are to be found in Ref. 7.

H. Flight Motor Characteristics

At the conclusion of the program, four flight motors have been cast and prepared for use. All flight motors are inspected by x-ray using the Allis-Chalmers 25-mev betatron at the Lockheed Propulsion Company. Exposures are made tangentially to the case ends to detect separation in highly stressed areas and radially through the grain to detect flaws.

The weight breakdown by subcomponents and axial center-of-gravity data representative of the final flight configuration are shown in Table 9. The predicted thrust delivered in the vacuum condition and the chamber-pressure history for an 80°F flight motor loaded with 60.5 lb of propellant are shown in Fig. 12.

Table 9. Typical flight motor weight and cg data

Component	Weight, lb	
Case	3.886	
Case insulation	1.896	
Nozzle	4.119	
Igniter	0.421	
Igniter nut, O-rings, studs	0.108	
Balance weights (typical)	0.032	
		10.462
Propellant (maximum)	60.94	
TOTAL		71.402
Axial cg measured from attachment plane		
Before propellant loading		8.4 in.
After propellant (max) loading		6.04 in.

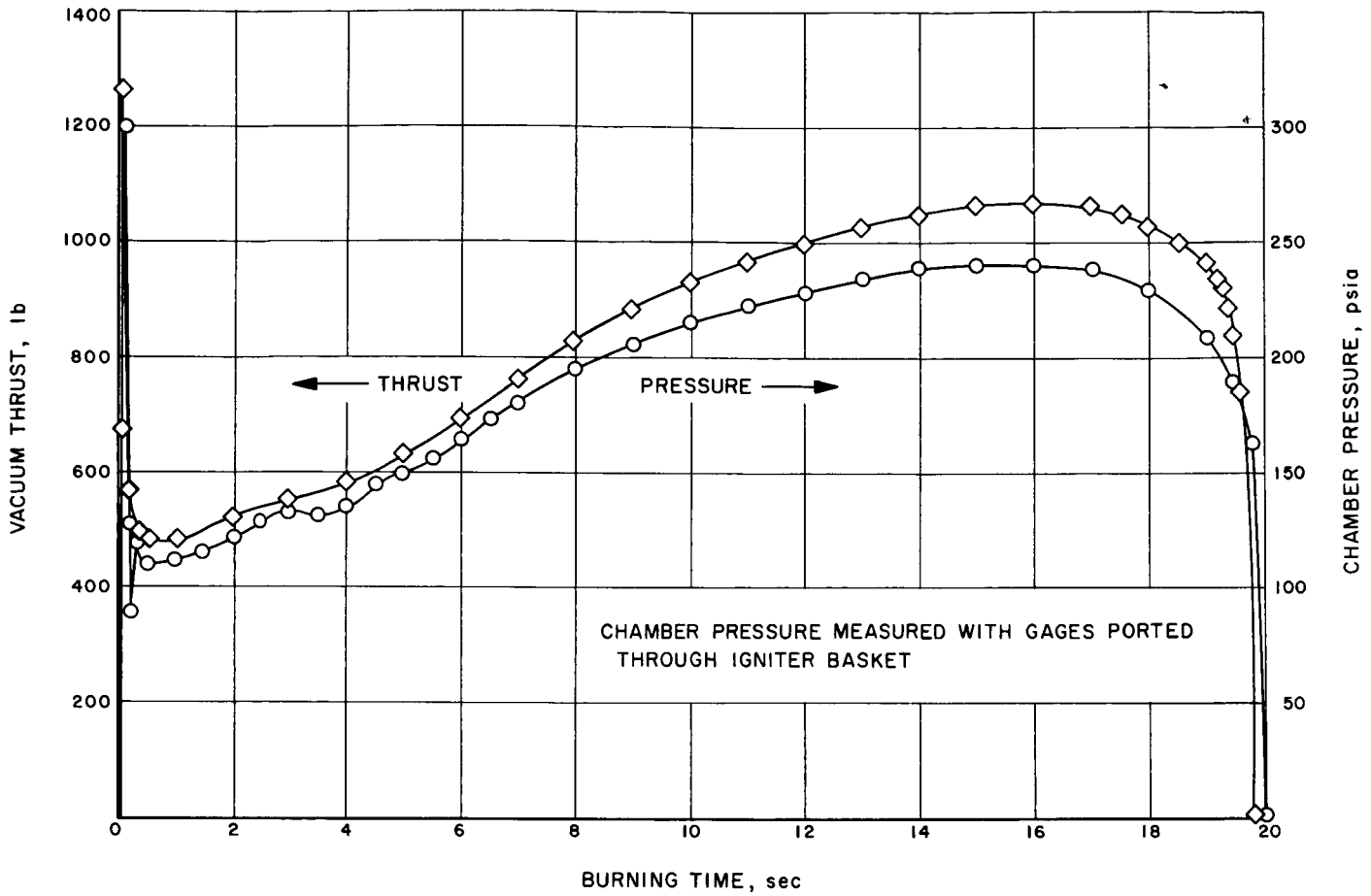

Fig. 12. Typical flight motor performance: Run AEDC-10

REFERENCES

1. *Space Programs Summary Nos. 37-13,* Vol. II, *37-14,* Vol. II; Vol. V of *37-15, 37-16, 37-17, 37-18, 37-19, 37-20,* Jet Propulsion Laboratory, Pasadena. (CONFIDENTIAL)

2. "First SYNCOM to test Synchronous Orbit," *Aviation Week and Space Technology,* August 20, 1962, pp. 80-89.

3. F. A. Anderson, *Properties and Performance of JPL 540 Propellant,* Technical Memorandum No. 33-131, Jet Propulsion Laboratory, Pasadena, May 1963. (CONFIDENTIAL)

4. *SYNCOM 1 Igniter Squib Development and Qualifications,* Technical Memorandum No. 33-132, Jet Propulsion Laboratory, Pasadena, May 1963.

5. *Six Component Thrust-Measuring System for Accurate Determination of Specific Impulse,* Technical Memorandum No. 33-23, Jet Propulsion Laboratory, Pasadena, August 19, 1960.

6. B. J. Lee, *Altitude Testing of the JPL Solid-Propellant Apogee Rocket Motor for the SYNCOM Spacecraft (Qualification Test Phase),* AEDC-TDR 63-15, Rocket Test Facility, AEDC, January 1963.

   B. J. Lee, *Altitude Testing of the JPL Solid-Propellant Apogee Rocket Motor for the SYNCOM Spacecraft (Preliminary Test Phase),* AEDC-TDR 62-214, Rocket Test Facility, AEDC, January 1963.

   C. F. Nokes, Jr., and A. F. Domal, *Altitude Testing of Two Modified JPL Solid-Propellant Rocket Motors for the SYNCOM Spacecraft,* AEDC-TDR 63-69, Rocket Test Facility, AEDC, April 1963.

7. "SYNCOM Solid-Propellant Rocket Motor Static Test Vibration Data," *Space Programs Summary No. 37-18,* Vol. IV, Jet Propulsion Laboratory, Pasadena.